Available online at www.sciencedirect.com
SCIENCE DIRECT®
ELSEVIER
Computers and Geotechnics 31 (2004) 285–300
COMPUTERS AND GEOTECHNICS
www.elsevier.com/locate/compgeo

Mandel–Cryer effects in fluid inclusions in damage-susceptible poroelastic geologic media

A.P.S. Selvadurai *, A. Shirazi

Department of Civil Engineering and Applied Mechanics, McGill University, 817 Sherbrooke Street West, Montreal, QC, Canada H3A 2K6

Received 8 October 2003; received in revised form 9 February 2004; accepted 26 February 2004
Available online 30 April 2004

Abstract

A fluid inclusion is an idealized form of a defect in a geomaterial. This paper examines the development and decay of pressure within a fluid inclusion, with a spheroidal shape, located in an extended fluid saturated poroelastic medium. In the modelling of the mechanical behaviour of the poroelastic solid, attention is also focused on the possible development of stress-induced damage that can alter the elasticity and permeability characteristics of the porous skeleton. The paper develops a computational approach to the study of the spheroidal fluid inclusion problem and examines the influence of the triaxial stress state, the geometry of the inclusion and damage-induced alterations of the poroelastic response on the celebrated Mandel–Cryer effect for a poroelastic solid. This effect relates to the delayed rise and decay of the fluid pressure in a poroelastic material subjected to three-dimensional stress states.

Keywords: Damage mechanics; Poroelastic damage; Biot consolidation; Mandel–Cryer effect; Permeability evolution; Spheroidal fluid inclusions; Stress state dependent damage

1. Introduction

Poroelasticity refers to the study of the mechanics of porous elastic materials that are saturated with compressible fluids. In classical poroelasticity, the elastic behaviour of the porous skeleton is assumed to be linear and the transport of the saturating compressible fluid through the pore space is governed by Darcy's law [1]. The classical theory is one of the noteworthy developments in continuum mechanics of multiphase media that has been successfully applied to examine time-dependent transient phenomena applicable to a variety of fluid-saturated geologic materials [2–13]. The assumption of linear elastic behaviour of the porous skeleton is recognized as a limitation in the applicability of the classical theory of poroelasticity to a wider class of geomaterials, with invariably non-linear phenomena in the constitutive response of the porous skeleton or the porous fabric. One way of overcoming this limitation is to incorporate elasto-plastic material behaviour in the constitutive response of the porous fabric. This type of approach has been successfully applied in the modelling of the consolidation behaviour of geomaterials such as soft clays and other saturated soils, which display distinct attributes of failure, described by criteria for initiation of failure and constitutive laws that govern the post-failure behaviour [11,14–18]. Of related interest are models of fluid-saturated media where changes in the constitutive properties are accounted for through changes in void ratio of the medium [12,19,20]. There are, however, other classes of geomaterials such as rocks and heavily over-consolidated geomaterials that tend to display brittle elastic behaviour. This can lead to the degradation in the elastic stiffness of the porous skeletal constitutive response. Stiffness degradations of this type can occur at stress states well below the combined stress states required to initiate complete failure or fracture of the porous skeleton in a brittle manner. This form of degradation can be a consequence of the development of micro-cracks and micro-voids in the porous fabric of the geomaterial, which would continue to maintain its elastic character. Accordingly, the behaviour lends itself

* Corresponding author. Tel.: +1-514-398-6672; fax: +1-514-398-7361.
E-mail address: patrick.selvadurai@mcgill.ca (A.P.S. Selvadurai).

0266-352X/$ - see front matter
doi:10.1016/j.compgeo.2004.02.008

to modelling through *continuum damage mechanics*. The damage evolution is assumed to maintain the applicability of both the linear elastic constitutive behaviour and Darcy's law, but a damage evolution law, formulated either through micro-mechanical considerations or obtained through experimental means, will now govern the evolution of the deformability and fluid transport parameters. The modelling of poroelastic behaviour of geomaterials by recourse to damage mechanics considerations is suggested by observations of the mechanical behaviour of brittle geomaterials such as granite, sandstone, claystone, limestone, etc., that exhibit elastic stiffness reductions and hydraulic conductivity increases well in advance of the pre-peak stress state. For example, the experimental investigations [21–26], point to the load-induced degradation of elastic moduli of rocks. The effect of micro-crack and micro-void generation on the evolution of hydraulic conductivity of saturated geomaterials has also been observed by [27–31]. This suggests the possibility of extending the classical theory of poroelasticity to include the effects of micro-void generation by appeal to a theory such as *continuum damage mechanics*. By adopting a damage mechanics approach, the influences of micro-void generation in the porous medium are accounted for in a phenomenological sense. The anisotropic damage model developed in [32] examines the poroelastic behaviour of saturated geomaterials, without consideration of hydraulic conductivity alteration during the damage process. The articles [33,34] document the computational modelling of the axisymmetric poroelastic contact problem where both elastic stiffness reduction and hydraulic conductivity alteration during damage evolution are considered. The former study deals with the purely axisymmetric computational modelling and the latter deals with a complete three-dimensional modelling of the axisymmetric contact problem.

In this paper we consider the problem of an extended, damage susceptible poroelastic medium, which is bounded internally by a fluid-filled cavity in the shape of a spheroid, or a *fluid inclusion*. The notion of a fluid inclusion can also be a model for a poroelastic region containing an excessively degraded but encapsulated intrusive zone with deformability characteristics substantially lower than those of the surrounding poroelastic medium and with permeability characteristics substantially higher than those of the surrounding poroelastic solid. Although such inclusion zones generally have a three-dimensional form, in this paper we model the fluid inclusion as either an oblate or a prolate spheroid. The damage susceptibility of the poroelastic medium takes into account both alterations in the *elastic stiffness* (usually a decrease) and the attendant alterations in the *permeability* (usually an increase). Also, such alterations are considered to be *non-reversible*. The poroelastic medium is subjected to a triaxial stress state in the far field. The application of this stress state induces pore pressures in the fluid within the cavity. With time, the pore pressure field in the cavity increases due to the compatible interactions between the pore fluid and the deformations of the porous solid skeleton. This phenomenon, the celebrated *Mandel–Cryer effect*, has been predicted both theoretically and observed experimentally for ideal poroelastic solids. The existence of the effect and its mathematical verification are given in articles [35,36], where the poroelastic response of a cubical element loaded under plane strain conditions is examined. The effect was also observed [37,38] in connection with the problem of a poroelastic sphere loaded by an external radial stress field with provision for complete fluid drainage at the boundary. The phenomenon also occurs in the mathematical modelling of the study of time lag in the pore pressure response in rigid porous piezometer tips embedded in poroelastic media [39,40]. Experimental verifications of the Mandel–Cryer effect have been observed in the response of saturated clay [41,42]. The physical explanation for the phenomenon is derived from the observation that in the initial stages of the poroelastic response, the volume changes associated with consolidation will occur almost invariably in regions at close proximity to surfaces that allow drainage. The reduction in volume of these regions due to consolidation results in a compression of the interior regions; this stressing action leads to the development of additional fluid pressures at the interior regions. The proof of the existence of the Mandel–Cryer effect in fluid inclusions in poroelastic media is therefore an outcome of these observations. Further references to studies in this area are given in the review articles cited previously [2,3]. The investigations in [37] point to the fact that the amplification and subsequent decay in the pore pressure depends on the elastic modulus and hydraulic conductivity characteristics of the poroelastic medium. It is therefore of interest to examine the extent to which the Mandel–Cryer effect can materialize in poroelastic media that are susceptible to damage, with time- and stress-dependent evolution of both the elastic stiffness of the porous skeleton and its permeability. This paper addresses this question through the computational modelling of the problem of an extended medium that is bounded internally by a fluid-filled spheroidal inclusion. The factors that are investigated include the triaxiality of the far field stress state, the stress state-dependency of the damage process, the influence of damage on the evolution of elastic stiffness and permeability characteristics and the shape of the spheroidal fluid inclusion in terms of its geometric aspect ratio. The accommodation of all these effects can be accomplished only through a computational scheme. Therefore the presentation of numerical results is restricted to specific situations that are sufficient to demonstrate key facets of the influence of damage evolution within the elastic range on the pressure generated in the fluid inclusion. Of related interest is the problem of a fluid-filled *spherical cavity* that was considered in [43], where the computational modelling of the problem was restricted to include only effects of an isotropic far-field stress state and without the consideration of the influence of stress state-dependency on the elastic stiffness and permeability evolution.

2. Classical poroelasticity

The constitutive equations governing the quasi-static response of a poroelastic medium consisting of a porous isotropic linear elastic soil skeleton saturated with a compressible pore fluid, take the forms

$$\boldsymbol{\sigma} = 2G\boldsymbol{\varepsilon} + \frac{2Gv}{(1-2v)}(\nabla \cdot \mathbf{u})\mathbf{I} + \alpha p\mathbf{I}, \tag{1}$$

$$p = \beta\zeta_{\mathrm{v}} + \alpha\beta(\nabla \cdot \mathbf{u}), \tag{2}$$

where $\boldsymbol{\sigma}$ is the total stress dyadic, p is the pore fluid pressure, ζ_{v} is the volumetric strain in the compressible pore fluid; v and G are the ''drained'' values of Poisson's ratio and the linear elastic shear modulus applicable to the porous fabric and $\mathbf{I}(= \mathbf{ii} + \mathbf{jj} + \mathbf{kk})$ is the unit dyadic. In (1), $\boldsymbol{\varepsilon}$ is the soil skeletal strain dyadic, defined by

$$\boldsymbol{\varepsilon} = \tfrac{1}{2}(\nabla\mathbf{u} + \mathbf{u}\nabla), \tag{3}$$

where $\mathbf{u}$ is the displacement vector and ∇ is the gradient operator. The material parameters α and β, which define, respectively, the compressibility of the pore fluid and the compressibility of the soil fabric, are given by

$$\alpha = \frac{3(v_{\mathrm{u}} - v)}{\widetilde{B}(1-2v)(1+v_{\mathrm{u}})} \quad \beta = \frac{2G(1-2v)(1+v_{\mathrm{u}})^2}{9(v_{\mathrm{u}} - v)(1-2v_{\mathrm{u}})}, \tag{4}$$

where v_{u} is the undrained Poisson's ratio and $\tilde{B}$ is the classical pore pressure parameter attributed to Skempton [44]. The effective stress dyadic $\boldsymbol{\sigma}'$ of the porous skeleton is given by

$$\boldsymbol{\sigma}' = \boldsymbol{\sigma} - \alpha p\mathbf{I}. \tag{5}$$

In the absence of body forces, the quasi-static equations of equilibrium for the complete fluid saturated porous medium take the form

$$\nabla \cdot \boldsymbol{\sigma} = \mathbf{0}. \tag{6}$$

The velocity of fluid transport within the pores of the medium is governed by Darcy's law,

$$\mathbf{v} = -\kappa\nabla p, \tag{7}$$

where $\mathbf{v}$ is the vector of fluid velocity and $\kappa(= k/\gamma_{\mathrm{w}})$ is the permeability, which is related to the hydraulic conductivity k and the unit weight of the pore fluid γ_{w} as indicated above. The mass conservation equation for the pore fluid can be stated as an equation of continuity, which, for quasi-static flows can be stated in the form

$$\frac{\partial\zeta_{\mathrm{v}}}{\partial t} + \nabla \cdot \mathbf{v} = 0. \tag{8}$$

Considering the thermodynamic requirements for a positive definite strain energy potential (see e.g. [45]) it can be shown that the material parameters should satisfy the following constraints:

$$G > 0; \quad 0 \leqslant \widetilde{B} \leqslant 1; \quad -1 < v < v_{\mathrm{u}} \leqslant 0.5; \quad \kappa > 0. \tag{9}$$

The governing equations for the displacement vector $\mathbf{u}$ and the scalar pore fluid pressure p can be reduced to the following:

$$G\nabla^2\mathbf{u} + \frac{\mu}{(1-2v)}\nabla(\nabla \cdot \mathbf{u}) + \alpha\nabla p = \mathbf{0}, \tag{10}$$

and

$$\kappa\beta\nabla^2 p - \frac{\partial p}{\partial t} + \alpha\beta\frac{\partial}{\partial t}(\nabla \cdot \mathbf{u}) = 0. \tag{11}$$

To complete the mathematical formulation of the initial boundary value problem it is necessary to prescribe boundary conditions and initial conditions applicable to the dependent variables $\mathbf{u}$ and p. The boundary conditions can be interpreted in terms of the conventional Dirichlet, Neumann or Robin boundary conditions. The systems of partial differential equations governing quasi-static poroelasticity are of the elliptic-parabolic type. The availability of a uniqueness of theorem [46] ensures that the classical poroelasticity problem is *well-posed* in a Hadamard sense.

3. Damage in poroelastic media

The classical theory of poroelasticity pre-supposes that the porous structure remains intact during deformations of the poroelastic skeleton. This is indeed a satisfactory and convenient assumption in many instances where the associated stress levels do not induce appreciable alterations in the poroelastic constitutive responses. The more extreme examples of alterations in the poroelastic behaviour can result from either the development of irreversible plastic deformations in regions of the porous soil skeleton to the development of discrete fractures, shear bands and discontinuities. These material alterations can introduce highly localized non-linear phenomena, accompanied by significant alterations in the fluid transport characteristics of the medium, particularly in the failure zones. While such processes can occur in geomaterials that are subjected to stress levels approaching the failure stress states [14,15,18], we are primarily concerned with geomaterials that maintain their *pre-dominantly elastic behaviour* but suffer some degree of micro-mechanical damage. A result of such damage can be the inhomogeneous alteration of the elastic behaviour of the porous skeleton and the attendant alteration in the material characteristics of the medium. Alterations of material characteristics can be introduced in zones of a poroelastic medium that experience continuum damage according to some prescribed damage evolution law. The mechanism that is most likely to lead to alterations in both the deformability characteristics and the permeability characteristics of a poroelastic medium, and at the same time maintain the elastic nature of the geomaterial skeletal response, is the creation of voids or cavities within the skeleton. The process of cavity generation in porous media is a phenomenological concept introduced to simplify a rather complicated set of processes associated with cavity nucleation, cavity expansion, cavity coalescence, etc. The creation of cavities is also largely governed by the stress state in the geomaterial skeleton, and the defects themselves can exhibit a directional dependence. The experimental evidence to date is insufficiently refined to support the development of any sophisticated theory to account for *directional dependency* in the defect evolution in a porous geomaterial fabric. Furthermore, the evolution of defects will occur in a medium that already has a void component. Therefore the meaningful introduction of a directional dependency in the created voids can be accomplished only by considering the characterization of the initial anisotropy of the pore space. The experimental verification of the pore space anisotropy is a difficult procedure that is certainly non-routine. The simplest approach for introducing the alterations in the elasticity and hydraulic conductivity of an initially porous geomaterial is to resort to the notion of *continuum damage mechanics*. The introduction of continuum damage mechanics is attributed to [47] and over the past four decades it has become is a well-researched area. The coupling of elasticity and damage modelling has been discussed by a number of researchers including, [33,48–55]. Attention is focused on the type of behaviour where the geomaterial experiences *isotropic damage* defined by a scalar damage variable D, which can be related to the initial area A_0 and the reduced area $\bar{A}$ through the relationship

$$D = \frac{A_0 - \bar{A}}{A_0}. \tag{12}$$

The damage variable varies between 0 and D_c, which is the critical value corresponding to the development of fracture of the material. (The critical damage parameter can be viewed as a normalizing parameter against which damage evolution can be estimated.) For isotropic damage, the net stress dyadic $\boldsymbol{\sigma}^n$ is related to the stress dyadic in the undamaged state $\boldsymbol{\sigma}$ according to

$$\boldsymbol{\sigma}^n = \frac{\boldsymbol{\sigma}}{(1-D)}. \tag{13}$$

Considering the 'strain equivalence hypothesis' proposed by [56], the constitutive equation for the damaged skeleton of the poroelastic medium can be written as

$$\boldsymbol{\sigma} = 2(1-D)G\boldsymbol{\varepsilon} + \frac{2(1-D)G\nu}{(1-2\nu)}(\nabla\cdot\mathbf{u})\mathbf{I} + \alpha p\mathbf{I}, \tag{14}$$

which implies the additional constraint that Poisson's ratio remains constant. The constitutive equation (14), however, does not take into consideration the influence of damage evolution on the pore pressure response that will result as a consequence of the evolution of additional void space. A modification to (14) can be of the form

$$\boldsymbol{\sigma} = 2(1-D)G\boldsymbol{\varepsilon} + \frac{2(1-D)G\nu}{(1-2\nu)}(\nabla\cdot\mathbf{u})\mathbf{I} + \alpha p(1+D)\mathbf{I}, \tag{15}$$

which accounts for the increase in surface area due to damage evolution. For the present, however, we shall restrict attention to the constitutive relationship defined by (14).

In addition to specifying the constitutive relations for the damaged geomaterial skeleton, it is also necessary to prescribe damage evolution criteria which can be postulated either by appeal to micro-mechanical considerations or determined from experiments. For example, based on a review of the results of experiments conducted on rocks, it has been shown [30] that

$$\frac{\partial D}{\partial \xi_d} = \eta\frac{\psi\xi_d}{(1+\xi_d)}\left(1-\frac{D}{D_c}\right), \tag{16}$$

where η and ψ are positive material constants and ξ_d is related to the second invariant of the deviator strain dyadic and given by

$$\xi_d = \tfrac{1}{2}[(\mathrm{tr}\mathbf{e})^2 - \mathrm{tr}\mathbf{e}^2], \quad \mathbf{e} = \boldsymbol{\varepsilon} - \tfrac{1}{3}\mathrm{tr}\boldsymbol{\varepsilon}\mathbf{I}. \tag{17}$$

The evolution of the damage variable can be obtained through an integration of (16) between limits D_0 and D where D_0 is the initial value of the damage variable corresponding to the intact state (e.g. D_0 is zero for materials in a virgin state). The deformability parameters applicable to an initially isotropic elastic material that experiences isotropic damage can be updated by

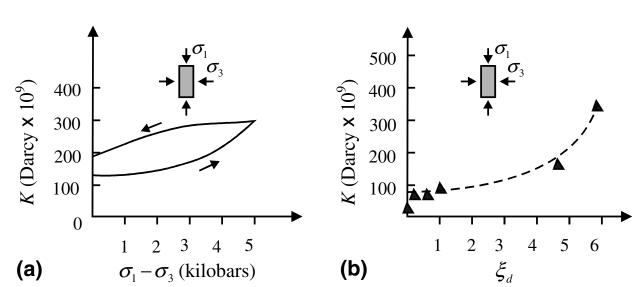

Fig. 1. Permeability evolution in saturated geomaterials: (a) after [27] and (b) after [28].

adjusting the elastic constants in the elasticity matrix $\mathbf{C}$ by its equivalent applicable to the damaged state $\mathbf{C}^{\mathrm{d}}$ but maintaining Poisson's ratio constant. Using the result (16), the evolution of D can be prescribed as follows:

$$D = D_{\mathrm{c}} - (D_{\mathrm{c}} - D_0)(1 + \psi\xi_{\mathrm{d}})^{\eta/\psi D_{\mathrm{c}}} \exp(-\eta\xi_{\mathrm{d}}/D_{\mathrm{c}}). \tag{18}$$

In relation to (14), the damage variable reflects the average material degradation, which accounts for an isotropic micro-scale effect, through a parameter that can be associated with a classical continuum formulation. For a brittle material, the damage variable can be obtained assuming the '*strain equivalence hypothesis*' and by using the stress–strain curve for a brittle geomaterial along with (14). The damage parameters η, ψ defined in (18) can also be obtained by correlating the damage variable D obtained from the stress–strain curve for a brittle geomaterial with respect to the

(I) Compute $I_1 = \varepsilon_{ii}$

(II) Check the criteria

$$I_1 < 0$$

No: Damage growth. Go to (III)

Yes: No further damage evolution. Use poroelastic parameters E, k with no more damage-induced modification. Go to (V).

(III) Compute D at Gauss integration points

$$D = D_C - (D_C - D_0)(1 + \psi\xi_d)^{\eta/\psi D_C} \exp(-\eta\xi_d / D_C)$$

$$\xi_d = (e_{ij}e_{ij})^{1/2}, \; e_{ij} = \varepsilon_{ij} - \frac{1}{3}\varepsilon_{kk}\delta_{ij}$$

(IV) Update the poroelastic parameters

$$E^d = (1 - D)E$$

$$k^d = (c_1 + c_2\varepsilon_d)k^0$$

or

$$k^d = (c_3 + c_4\xi_d{}^2)k^0$$

(V) Solve the governing equations for u_t, p_t and calculate the strain tensor

$$\varepsilon_{ij} = \frac{1}{2}(u_{i,j} + u_{j,i})$$

(VI) Check the criteria

$$D \geq D_C$$

No: Damage growth. Return to (I).

Yes: No further damage evolution. Exit.

Fig. 2. Computational algorithm for stress state-dependent evolution of damage in the poroelastic medium.

equivalent shear strain. When damage in poroelastic media results in the creation of defects such as micro-cracks and micro-voids, it is likely that these defects will also lead to alterations in the permeability characteristics of the poroelastic medium. The literature on permeability evolution in porous media tends to focus on experimental evaluation of alteration in the permeability of geomaterials subjected to conventional triaxial stress states. Results of permeability experiments conducted on granite are documented in [27]. The results of permeability tests conducted on sandstone [28] are shown in Fig. 1. The experimental results given in [29] also indicate permeability alterations in granite with an increase in stress/strain; it is not altogether clear whether such observations could be attributed to alterations occurring predominantly in strain localizations zones.

In studies conducted to examine the indentation of a damage-susceptible poroelastic halfspace by a rigid cylindrical indenter with a flat base, the following expressions was proposed [33] for the evolution of permeability κ (expressed in m^2) as a function of the parameter ξ_d;

$$\kappa^{d} = \left(1 + \tilde{\beta}\xi_{d}^{2}\right)\kappa^{0}, \tag{19}$$

where $\tilde{\beta}$ is a constant and κ^0 is the permeability of the undamaged material. The quadratic-dependency of the permeability on ξ_d is a plausible estimate that can be substantiated particularly through the results for sandstone given in [28] and adopted here, strictly for purposes of the exercise in computational modelling.

4. Computational modelling

The finite element method has been widely applied for the analysis of problems in the classical theory of poroelasticity and complete discussions of the computational aspects of poroelasticity are given in articles [5,6,11,57–60]. The Galerkin approximation technique is applied to transform the partial differential equations into a discretized matrix form giving rise to the following incremental forms for the equations governing poroelastic media:

$$\begin{bmatrix} \mathbf{K} & \mathbf{C} \\ \mathbf{C}^{T} & \{-\gamma\Delta t\mathbf{H} + \mathbf{E}\} \end{bmatrix} \begin{Bmatrix} \mathbf{u}_{t+\Delta t} \\ \tilde{p}_{t+\Delta t} \end{Bmatrix} = \begin{bmatrix} \mathbf{K} & \mathbf{C} \\ \mathbf{C}^{T} & \{(1-\gamma)\Delta t\mathbf{H} + \mathbf{E}\} \end{bmatrix} \begin{Bmatrix} \mathbf{u}_{t} \\ \tilde{p}_{t} \end{Bmatrix} + \{\mathbf{F}\}, \tag{20}$$

where **K** is the stiffness matrix of the solid skeleton; **C** is the stiffness matrix due to interaction between the solid skeleton and the pore fluid; **E** is the compressibility matrix of the pore fluid; **H** is the permeability matrix; **F** are force vectors due to external tractions, body forces and flows; $\mathbf{u}_t$ and p_t are, respectively, the nodal displacements and the pore pressure at time t; and Δt is the time increment. The time-integration constant γ varies between 0 and 1. The criteria governing stability of the integration scheme given by [58] requires that $\gamma \geqslant 1/2$. Investigations documented in [11] and [60] suggest that the stability of the solution can be achieved by selecting values of γ close to unity.

For the analysis of the poroelasticity problem that incorporates influences of damage evolution, an incre-

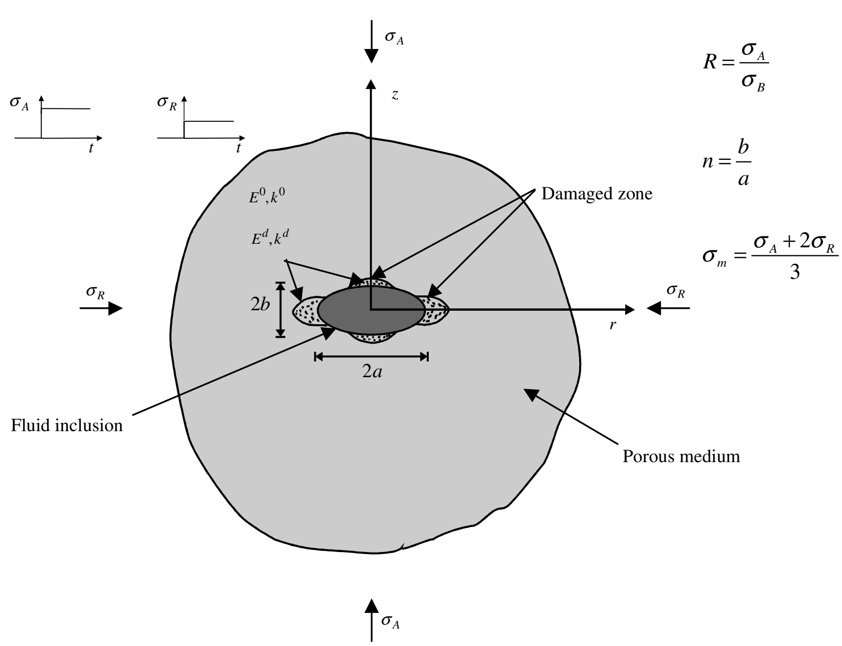

Fig. 3. Oblate spheroidal fluid inclusion in an extended poroelastic medium.

mental finite element procedure is developed, along the lines outlined in [33]. This procedure accounts for the alterations in both hydraulic conductivity and elasticity parameters. It must be remarked that although there are formal similarities between the hypoelastic non-linear approach [15,61,62] and the damage-induced degradation of the elasticity properties, the procedures used here are within the context of a *coupled fluid flow-mechanical deformation* problem, which requires the evaluation of both stress and time dependent evolution of both the elasticity and fluid transport characteristics of the medium. Furthermore we can identify two approaches to accommodate the influences of damage evolution; the first allows damage-induced evolution of the elasticity and hydraulic conductivity to be *independent of the "sense"* of the stress state as defined by the compressive or tensile character of the principal stresses, and governed by the damage and permeability evolution criteria described previously by (18) and (19) respectively. The constitutive matrix **C** and the per-

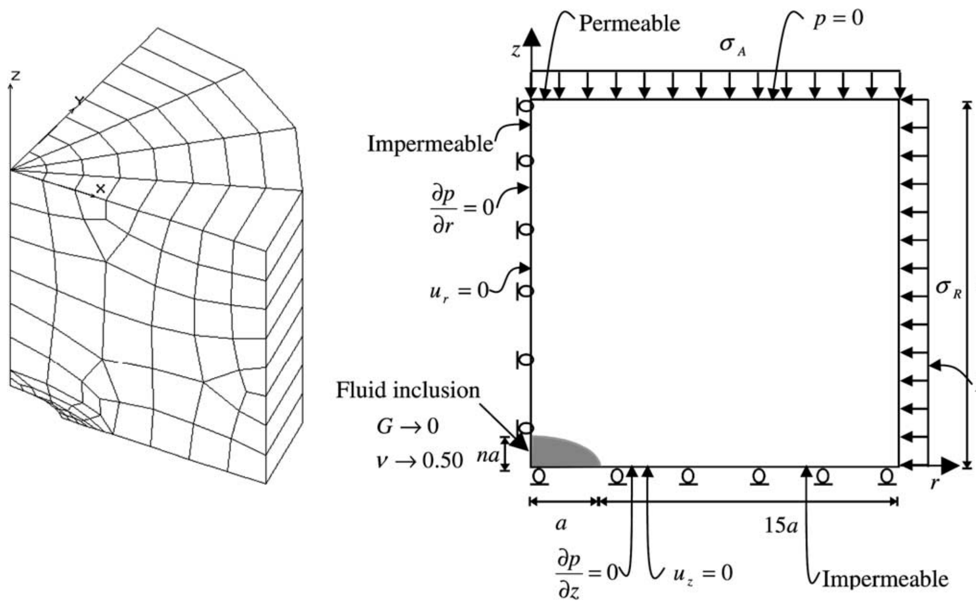

Fig. 4. Finite element discretization of the damage susceptible poroelastic medium bounded internally by an oblate spheroidal fluid inclusion: geometry and boundary conditions.

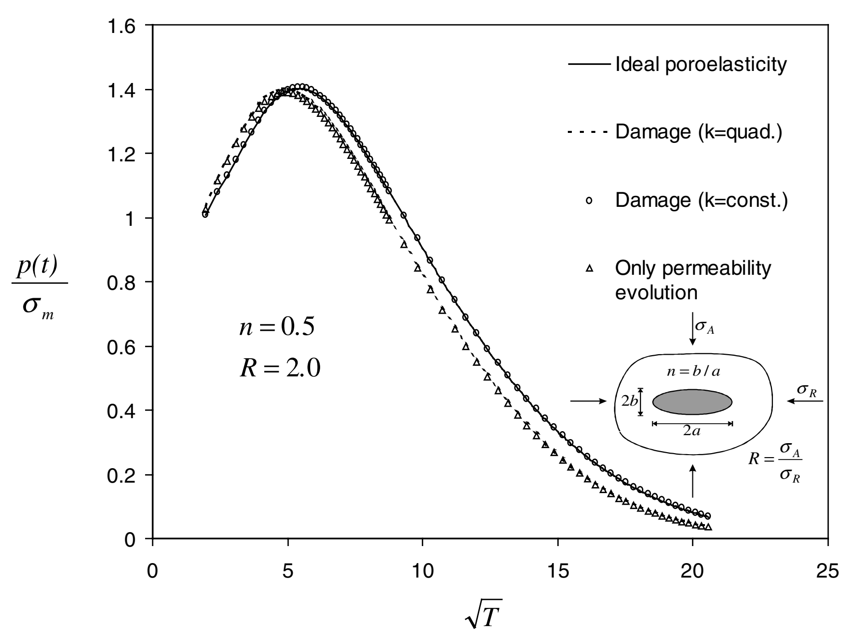

Fig. 5. Evolution of fluid pressure in the oblate spheroidal fluid inclusion in a non-isotropic far field stress field: Comparison of results for the damaged and ideal poroelasticity material responses ($n = 0.5$) (*stress state-independent damage evolution*).

meability κ are updated at the integration points, at each time step, to account for evolution of damage. The discretized forms of the governing equations are then solved to obtain the state of strain at each integration point using the updated values of these, denoted by $\mathbf{C}^{\mathrm{d}}$ and κ^{d}, respectively. An iterative procedure that uses a standard Newton–Raphson technique is employed to solve the coupling between the state of strain and the extent of damage at each step. The convergence criterion adopted in the analysis is based on the norm of the evolution of the damage variable in relation to a prescribed tolerance [49]. De-

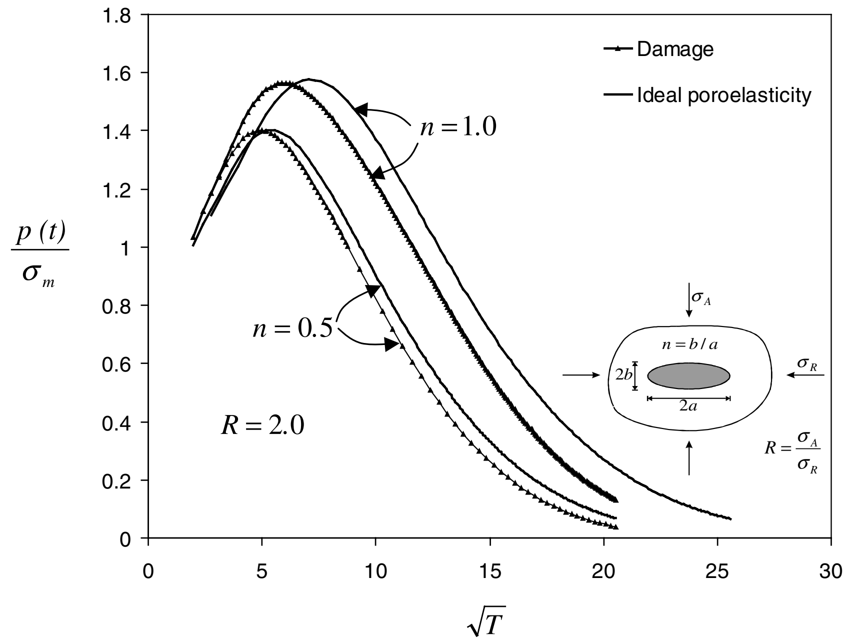

Fig. 6. Evolution of fluid pressure in the oblate spheroidal fluid inclusion in a non-isotropic far field stress field: comparison of results of the damaged and ideal poroelasticity material responses ($n = 0.5; 1.0$) (*stress state-independent damage evolution*).

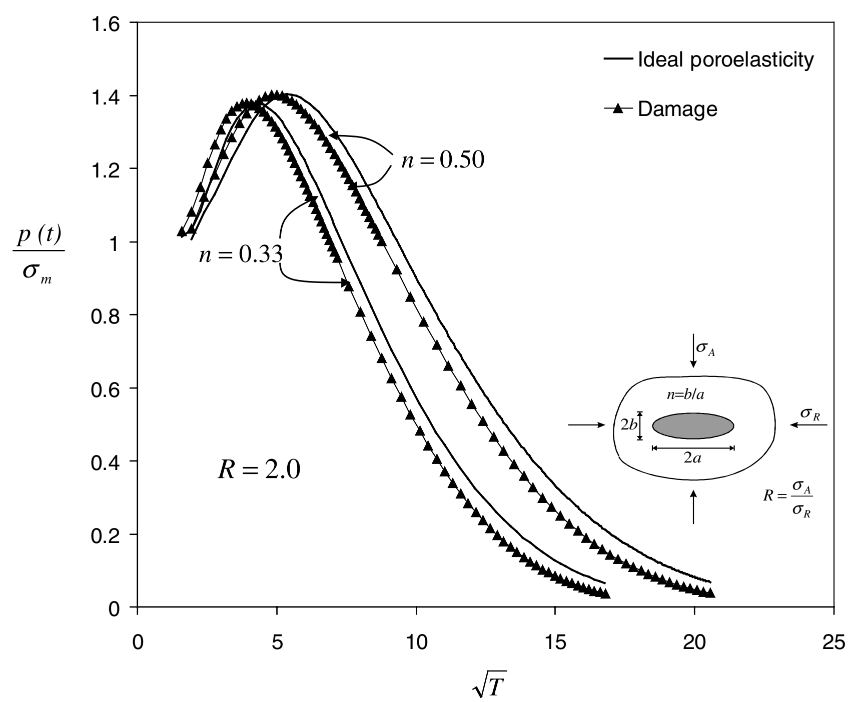

Fig. 7. Evolution of fluid pressure in the oblate spheroidal fluid inclusion: influence of the geometry of the oblate spheroidal inclusion in a non-isotropic far field stress field (*stress state-independent damage evolution*).

tails of the iterative procedure and the associated numerical algorithm are summarized by [33]. In the second approach we assume that the damage evolution is *dependent on the sense of stress state* as defined by the various combinations of the principal strains. For example, it is foreseeable that the process of void and defect development in the poroelastic fabric is enhanced when the triaxial stress state is tensile and that

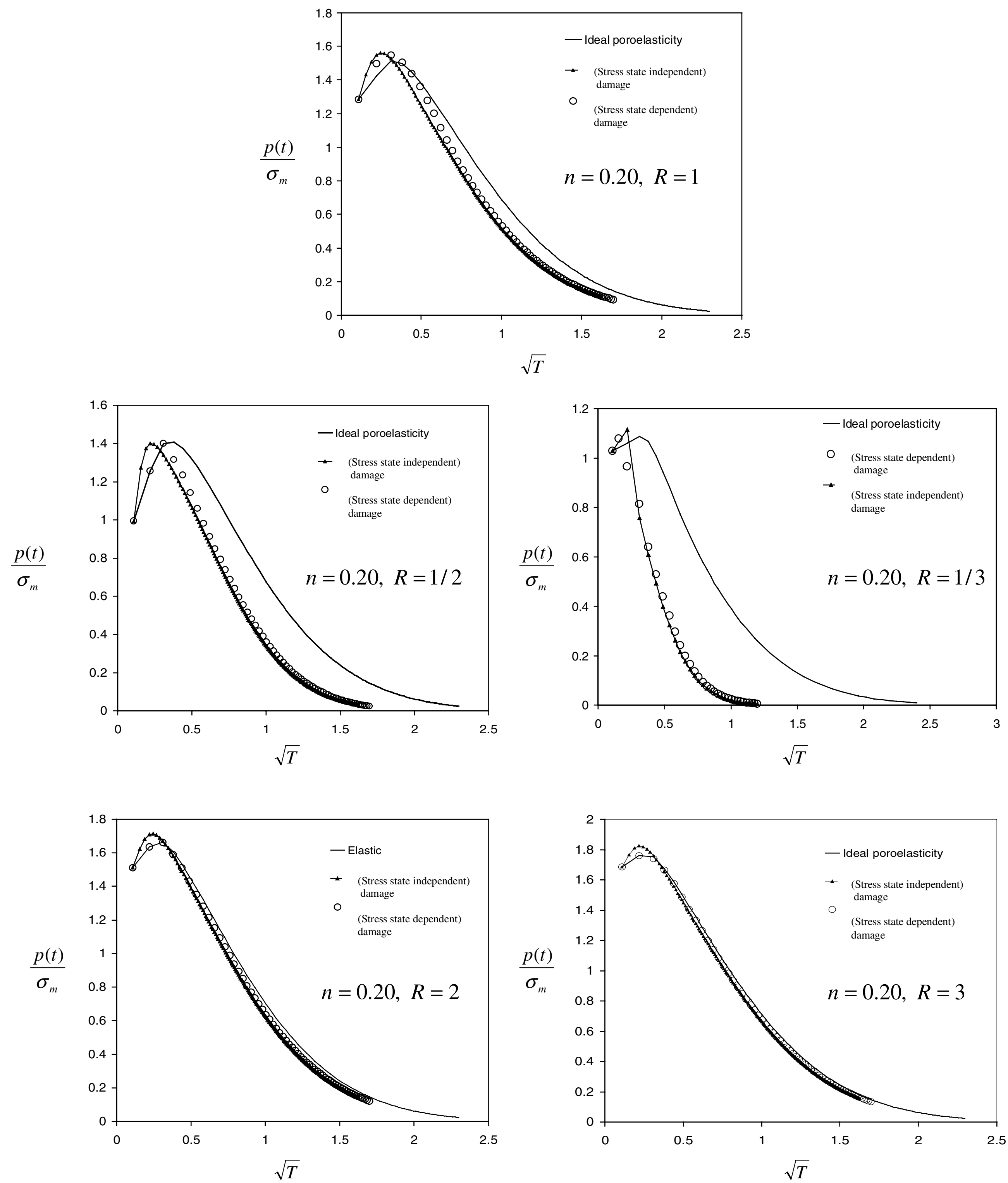

Fig. 8. Evolution of fluid pressure in the oblate spheroidal fluid inclusion in a non-isotropic far field stress with different deviatoric stress ratios (*stress state-dependent damage evolution*) ($R = \sigma_A/\sigma_R$; $n = b/a$; $\sigma_m = (\sigma_A + 2\sigma_R)/3$).

such effects can be suppressed when the stress state is compressive. Other combinations of principal stresses, involving tensile and compressive stresses can induce different magnitudes of damage evolution. Just as in the development of yield criteria for geomaterials, the characterization of stress state-dependent damage requires the experimental determination of the material response to differing stress or strain paths. Experimental verifications of the stress-dependent damage evolution in geomaterials are scarce, in the sense that the database is insufficient to develop a comprehensive theory applicable to the class of brittle geomaterials of special interest to this paper. However, this limited data does point to the observation that damage can increase when the material experiences a volume expansion [63]. A plausible approximation is therefore to assume that damage will initiate when the strain state satisfies the criterion

$$I_1 = \mathrm{tr}\boldsymbol{\varepsilon} > 0, \tag{21}$$

where tensile strains are considered to be positive. These two procedures can be regarded as two limiting responses associated with the damage-induced evolution processes.

In contrast to the deterioration of elastic properties during damage evolution under tensile loadings, there is also the possibility that the elasticity properties will be enhanced of as a result of void reduction or void closure during compressive loading of the poroelastic medium. Such phenomena have been observed during experiments conducted on materials such as granite [64]. The enhancement of the elastic properties is most likely to occur when the defects have an elongated form such as cracks or flattened cavities. This will also require the consideration of the effects of oriented defects, which is beyond the scope of the present paper. Since attention is directed to the isotropic idealization of damage modelling, we restrict attention to damage enhancement for all states of strain that satisfy (21) and assume that the porous fabric remains intact for any other state of strain. Admittedly, this is only a plausible approximation, but since the intention of this study is to gain some insight into the stress state-dependency of damage evolution on the poroelastic response of the fluid inclusion, the simplified assumption (21) is justifiable. Another objective of the paper is to conduct a comparison of results for the pore pressure response of the fluid inclusion for the different types of damage development scenarios, so that attention is restricted to this relatively elementary representation of stress state-dependent damage and its influence on the evolving deformability and permeability characteristics of the porous fabric of the poroelastic medium. It should also be noted that the alterations in the deformability and permeability properties of the porous skeleton achieved through damage evolution are considered to be non-reversible (i.e. during any time in the poroelastic analysis, the *lowest value of the deformability* and the *highest value of the permeability* governs the incremental poroelastic response). The basic computational algorithm used in the numerical computations is shown in Fig. 2. Again, the convergence criterion adopted for the termination of the computations is based on the norm of the evolution of the damage variable in relation to a prescribed tolerance.

5. The spheroidal fluid inclusion problem

We examine, separately, problems related to *oblate* and *prolate* spheroidal fluid inclusions located in an extended damage-susceptible poroelastic medium and

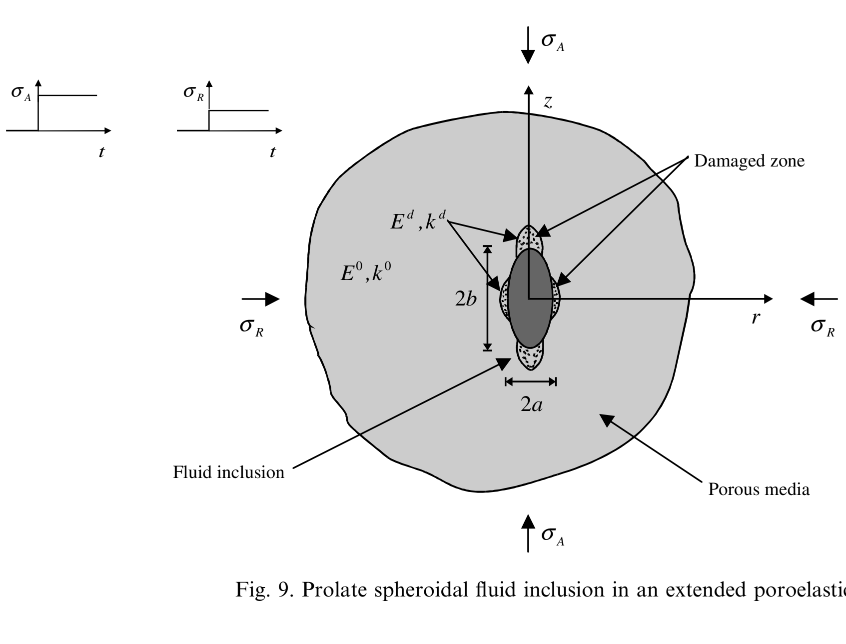

Fig. 9. Prolate spheroidal fluid inclusion in an extended poroelastic medium.

subjected to a triaxial state of stress defined by a far-field axial stress of σ_A and a far field radial stress of σ_R. Both these stresses have a time-dependency that can be characterized by a Heaviside step function of time. The pore fluid pressures in the far field are maintained at zero and attention is focused on the computational evaluation of the *excess fluid pressure generation and decay* in the spheroidal fluid inclusion as a result of (i) damage-induced alterations of the elastic properties and/or the fluid transport characteristics of the geomaterial skeleton, (ii) influence of stress state-dependent damage evolution, (iii) the influence of the anisotropy in the far-field stress state, and (iv) the geometric aspect ratio of the spheroidal fluid inclusion. For the purposes of the computational modelling, we select sandstone as the damage-susceptible poroelastic material with the following properties [32]:

Elasticity parameters: $E = 8300$ MPa; $\nu = 0.195$; $\nu_u = 0.4999$,

Failure parameters: $\sigma_C = 30$ MPa (compressive); $\sigma_T = 3$ MPa (tensile),

Damage parameters: $\psi = \eta = 130$; $D_C = 0.75$,

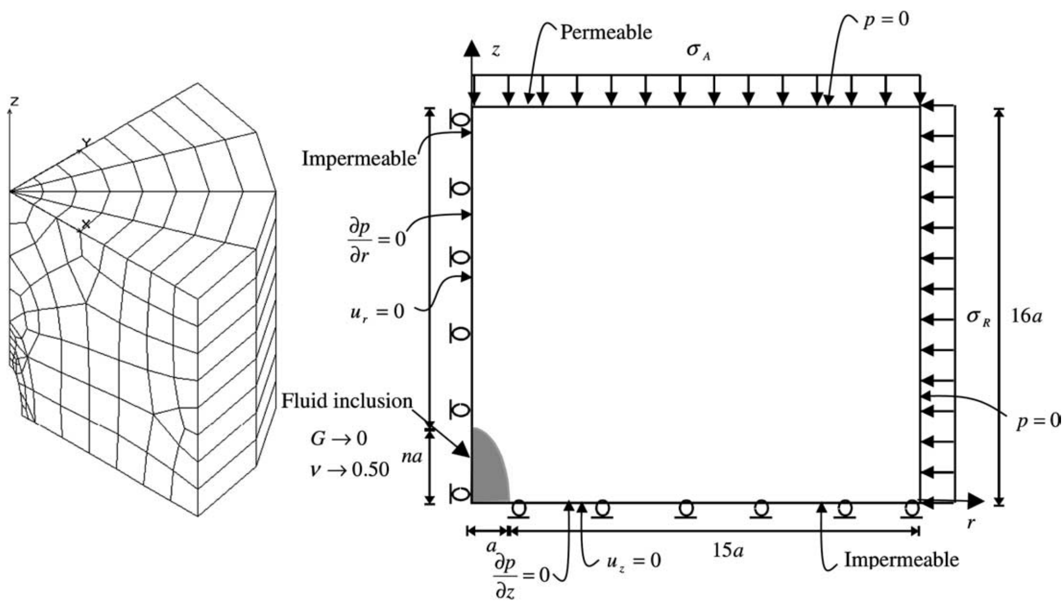

Fig. 10. Finite element discretization of the damage susceptible poroelastic medium bounded internally by a prolate spheroidal fluid inclusion: geometry and boundary conditions.

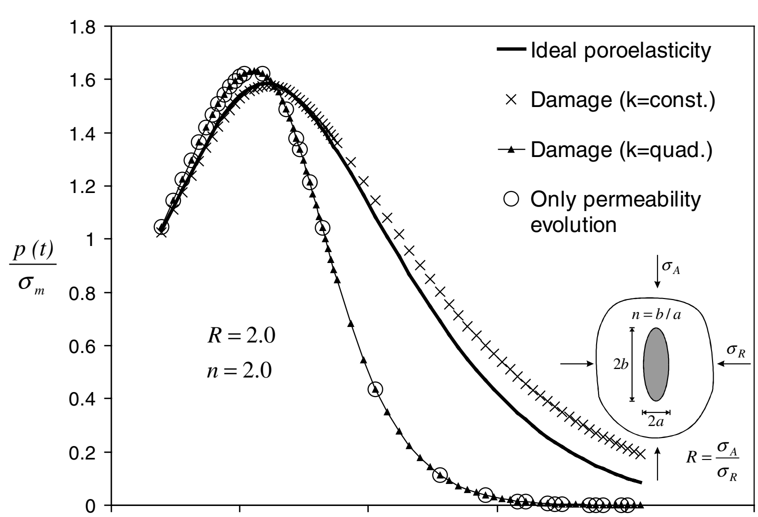

Fig. 11. Fluid pressure for prolate fluid inclusion in a non-isotropic stress field ($n = 2.0$) (*stress state-independent damage evolution*).

Fluid transport parameters: $k_0 = \kappa_0\gamma_w/\mu_v = 10^{-6}$ m/s; $\tilde{\beta} = \beta \times 10^5$; $\beta = 3$,
where γ_w is the unit weight of water and μ_v is the dynamic viscosity of the fluid.

Ideally, the computational model of the fluid inclusion should be represented as a fluid element with incompressible behaviour. This entails the re-formulation of the computational procedure to account for the fluid response. The procedures for the implementation of the fluid element are available in the literature [65]. In this study, however, the fluid inclusion is modelled by considering an alteration in the poroelasticity parameters applicable to the inclusion region. This is considered sufficient for purposes of illustrating the overall response

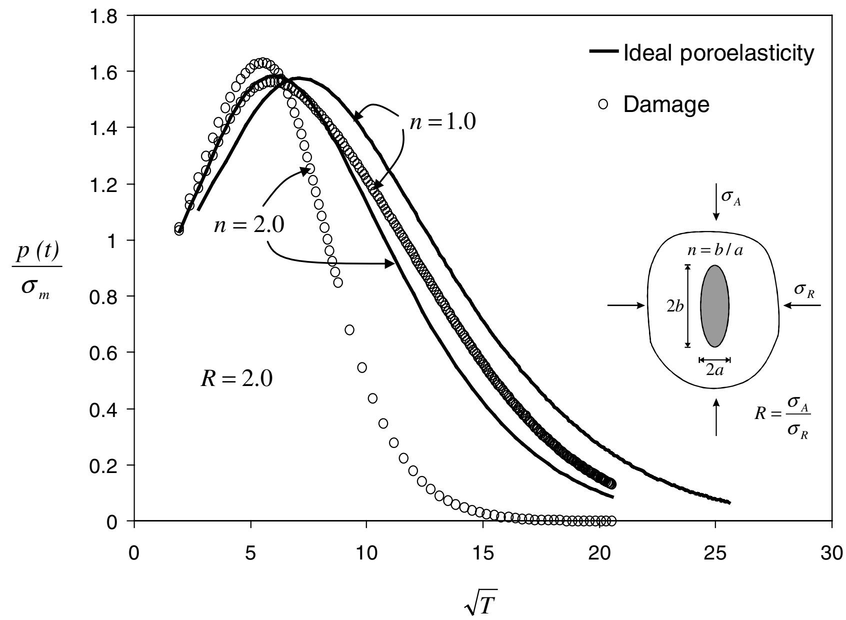

Fig. 12. Evolution of fluid pressure in the prolate spheroidal fluid inclusion: influence of the geometry of the prolate spheroidal inclusion in a non-isotropic far field stress field (*stress state-independent damage evolution*).

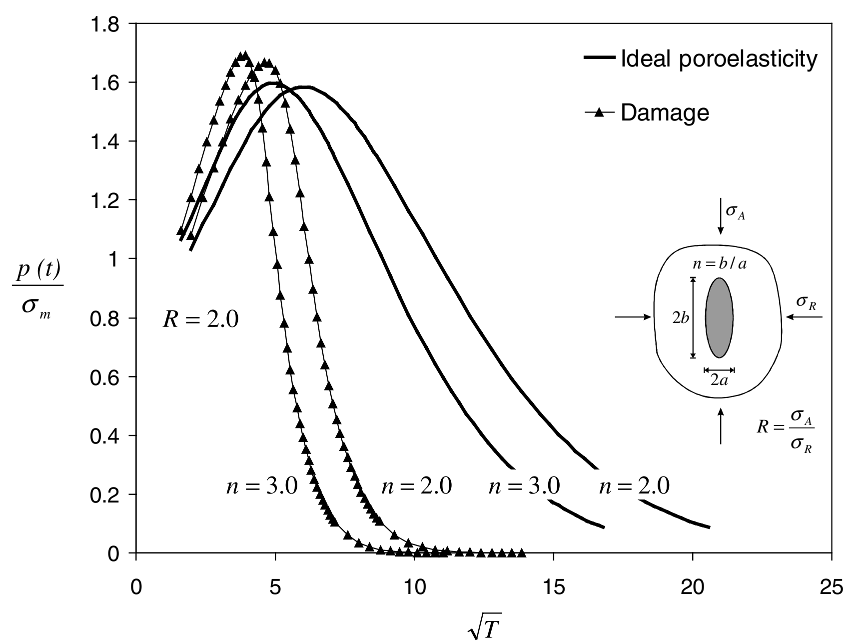

Fig. 13. Evolution of fluid pressure in the prolate spheroidal fluid inclusion: influence of the geometry of the prolate spheroidal inclusion in a non-isotropic far field stress field (*stress state-independent damage evolution*).

of the fluid inclusion. Accordingly, the inclusion is modelled as a non-damage-susceptible poroelastic medium with a relatively low shear modulus (low in relation to the surrounding poroelastic medium) and a relatively high hydraulic conductivity. The specific values of the poroelastic parameters chosen to model the fluid inclusion are as follows:

Elasticity parameters: $G = 1$ MPa; $\nu_f = 0.4999$,
Fluid transport parameters: $k_0 = \kappa_0\gamma_w/\mu_v = 10^{-3}$ m/s.

These values give a nearly uniform time-dependent fluid pressure variation within the inclusion region, to within an accuracy of 2% in the spatial variation. These fluid pressures are determined using the pore fluid pressures calculated at the specific locations of the element that are applicable to the poroelastic element. A reduction of G by an order of magnitude and the increase in k_0 by an order of magnitude does not result in a noticeable change in the computed fluid pressures. The computa-

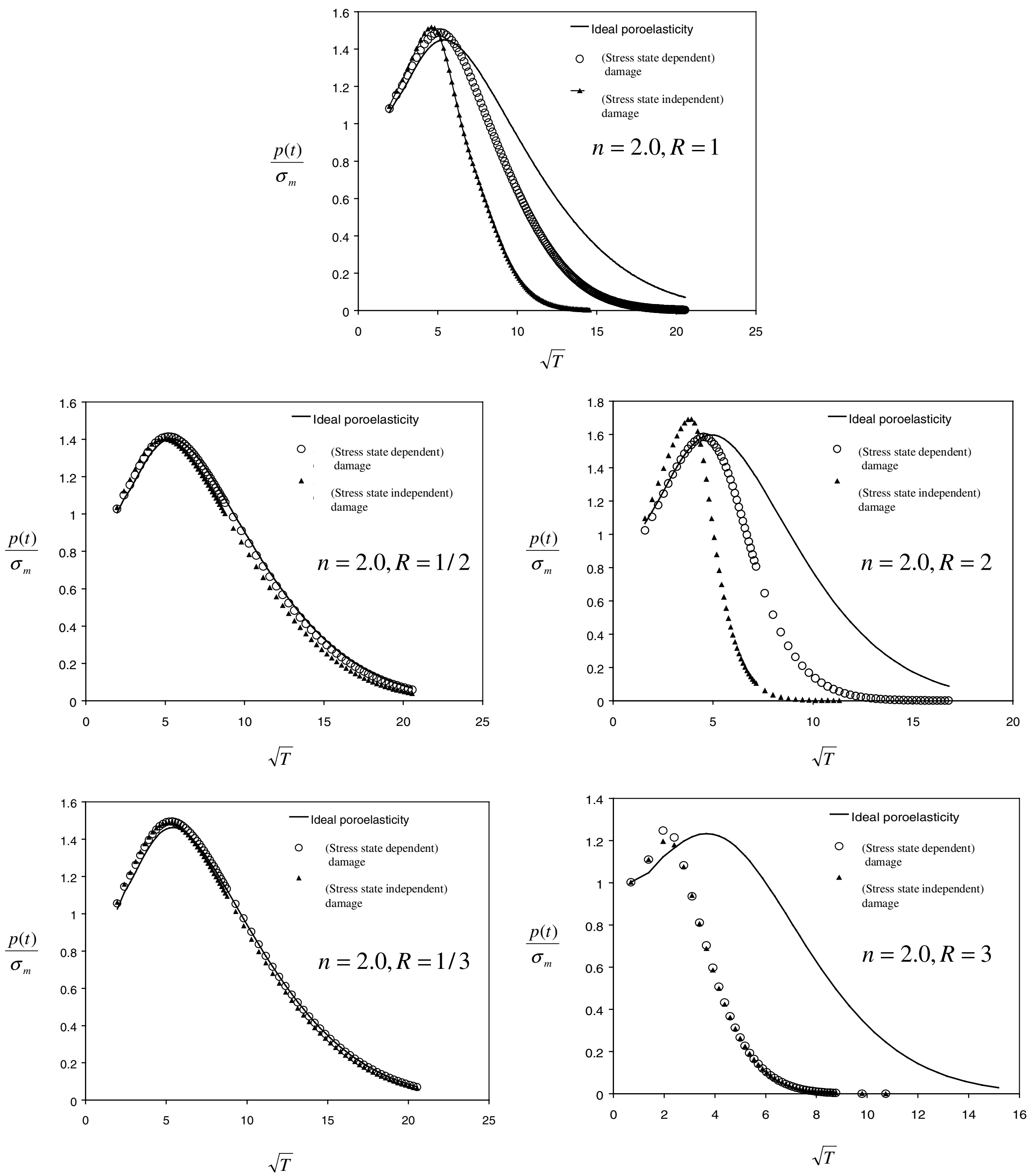

Fig. 14. Evolution of fluid pressure in the prolate spheroidal fluid inclusion in a non-isotropic far field stress with different deviatoric stress ratios (*stress state-dependent damage evolution*) ($R = \sigma_A/\sigma_R$; $n = b/a$; $\sigma_m = (\sigma_A + 2\sigma_R)/3$).

tional results are verified at each stage to ensure that all points within the inclusion have the same fluid pressure at any given time.

5.1. The oblate spheroidal fluid inclusion

We first consider the problem of an extended, damage-susceptible poroelastic medium bounded internally by an oblate spheroidal fluid-filled cavity (Fig. 3). The poroelastic medium is subjected to a far-field tri-axial stress state defined by an axial stress σ_A and radial stress σ_R that are each defined by a Heaviside step function of time. Fig. 4 illustrates a typical three-dimensional finite element discretization used in the finite element code developed for this research and the associated boundary conditions employed in the computational modelling of the oblate fluid inclusion problem. The finite element mesh is refined all around the inclusion in order to model the variations in material parameters of the media more accurately. Figs. 5–7 illustrate the range of responses for the time-dependent evolution and decay of the pressure in the oblate fluid inclusion for the cases where the extended medium exhibits (i) ideal poroelasticity, (ii) poroelasticity with stress state-independent damage that results in either alteration in the elastic stiffness or permeability characteristics or the alteration of both elasticity and permeability characteristics of the poroelastic medium, and (iii) the geometry of the oblate spheroidal fluid inclusion. These results demonstrate the significant influence of the evolution of permeability in the poroelastic medium on both the amplification and decay of the pressure in the fluid inclusion. The results also indicate that the geometry of the fluid inclusion influences the amplification and decay in the fluid pressure. As the oblate spheroid flattens, or as $n = b/a$ becomes small, the changes to the elastic stiffness and permeability characteristics of the poroelastic medium induced by stress magnification in regions of high boundary curvature of the inclusion results in both a more rapid generation of the peak fluid pressure and its decay. Fig. 8 presents comparisons for the pressure decay in a flattened oblate spheroidal fluid inclusion corresponding to poroelastic materials that display *stress state-dependent* and *stress state-independent* damage phenomena and for a range of values of the parameter R that accounts for the non-isotropy of the far-field stress state. It is evident that for the fluid inclusion with an oblate spheroidal shape, the influence of the non-isotropy in the far field stress state on the pressure decay response increases as R decreases.

5.2. The prolate spheroidal fluid inclusion

The computational modelling is now applied to examine the problem of an extended poroelastic medium, bounded internally by a prolate or an elongated fluid inclusion (Fig. 9). A typical three-dimensional finite element discretization of the poroelastic domain used in the computational modeling of the prolate fluid inclusion problem is shown in Fig. 10. Figs. 11–13 show the time-history of pressure development in the prolate fluid inclusion for the cases where the poroelastic medium exhibits (i) ideal poroelasticity, (ii) poroelasticity with stress state-independent damage resulting in either alteration in the elastic stiffness or permeability characteristics or alteration of both elasticity and permeability characteristics of the poroelastic medium, and (iii) the geometry of the prolate spheroidal fluid inclusion. Again, these results indicate the relative importance of the influence of the elastic stiffness reduction, permeability enhancement and variations in the geometry of the elongated spheroid, on the pore fluid pressure evolution in the elongated fluid inclusion. As the prolate fluid inclusion approaches a needle-shape, both the time to attain peak fluid pressure and the time for complete dissipation of the fluid pressures that are generated are reduced. In Fig. 14 the results demonstrate the influence of the non-isotropy of the far-field stress state on the generation and decay of the pressure in the fluid inclusion. As the far-field axial stress σ_A increases in relation to the far-field radial stress σ_R, the time to attain the peak fluid pressure in the damage-induced cavity and the time for decay of this fluid pressure are both considerably reduced. In contrast to the results obtained for the oblate or flattened spheroid, the influence of the non-isotropy of the far-field stress state is dominant when the R increases. Again, the stress magnification that results from both the shape of the inclusion and the axial stress state contributes to increased damage in the highly stressed regions thereby altering the amplification and decay processes of the pressure in the fluid inclusion.

6. Concluding remarks

The development of mechanical damage in fluid-saturated porous geomaterials is of considerable interest in many geomechanics and geoenvironmental applications. In contrast to complete failure of the geomaterial, the development of damage in a fluid-saturated brittle geomaterial usually results in the reduction in its *elasticity characteristics* and an attendant increase in the *permeability characteristics*. In fluid-saturated porous geologic media, these alterations directly influence the coupling processes and consequently the time-dependent response of the poroelastic geomaterial. The theory of continuum damage mechanics offers a convenient framework for examining the influences of pre-peak damage evolution on the mechanics of the poroelastic medium. This paper considered problems of idealized spheroidal fluid inclusions, demonstrating the influences of damage-induced evolution of elasticity and permeability on the pressure transients in such fluid inclusions. The choice of the fluid inclusion problem is dictated by the possibility of observing the delayed fluid pressure rise in the damage susceptible poroelastic medium as documented, in classical poroelasticity, by the Mandel–Cryer effect. The computational modelling of the fluid inclusion problem is achieved through consideration of plausible criteria, available in the literature, for the evolution of both the elasticity and permeability characteristics. It is shown that the pressure transients that develop in the fluid-filled inclusion can be significantly influenced by the evolution of damage and the accompanying alterations in the elasticity and permeability characteristics of the deformable porous medium, the geometry of the inclusion and the non-isotropy of the far-field stress state. The most noticeable effect is the rapid decay experienced by the pressure in the fluid inclusion when permeability evolves with damage. In a sense this is to be expected; the investigation, however, presents a methodology for an assessment of the phenomenon. This observation has important implications to other areas of application; for example, the mechanics of fault regions and other discontinuities in fluid-saturated brittle geologic media can be influenced by micro-mechanical damage initiated in the vicinity of the discontinuity, leading to the modification of the fluid pressure response in the contact zone [7,8,66]. This can inhibit the generation of excessive fluid pressures in geomaterial discontinuities and lead to an enhancement in the stability of the discontinuity. Further applications of the influence of damage-induced mechanics on poroelastic problems of a geomechanical nature could arise in the study of tunnels, shafts, excavations and other openings in fluid-saturated geomaterials, where the time-dependent effects can have an influence on both the deformations and stability of such facilities.

Acknowledgements

The work described in this paper was supported in part by an operating research grant awarded by the Natural Sciences and Engineering Research Council of Canada awarded to the first author. The authors are grateful to the referees for their interest in the paper and for their constructive comments.

References

[1] Biot MA. General theory of three-dimensional consolidation. J Appl Phys 1941;12:155–64.
[2] Schiffman RL. A bibliography on consolidation. In: Corapcioglu MY, Bear J, editors. Fundamentals of transport phenomena in porous media. The Netherlands: Martinus Nijhoff Publishers; 1984. p. 617–69.
[3] Detournay E, Cheng AH-D. Fundamentals of poroelasticity. Comprehensive rock engineering principles, practice and projects. In: Fairhurst C, editor. Analysis and design methods, vol. II. Oxford: Pergamon Press; 1993. p. 113–71 [Chapter 5].
[4] Coussy O. Mechanics of porous media. New York: John Wiley; 1995.
[5] Selvadurai APS, editor. Mechanics of poroelastic media. Dordrecht, The Netherlands: Kluwer Academic Publishers; 1996.
[6] Selvadurai APS. On some recent developments in poroelasticity. In: Desai CS, editor. IACMAG 2001, Proceedings of the 10th International Conference on Computing Methods in Advanced Geomechanics, Tucson, Arizona, vol. 2. The Netherlands: A.A. Balkema; 2001. p. 1761–9.
[7] Rudnicki JW. Boundary layer analysis of plane strain shear cracks propagating steadily on an impermeable plane in an elastic diffusive solid. J Mech Phys Solids 1991;39:201–21.
[8] Rudnicki JW. Moving and stationary dislocations in poroelastic solids and applications to aseismic slip in the earth's crust. In: Selvadurai APS, editor. Mechanics of poroelastic media. Kluwer Academic Publishers: The Netherlands; 1996. p. 3–22.
[9] Cheng AH-D, Detournay E, Abousleiman Y. (Eds.). Poroelasticity. Maurice A. Biot Memorial Issue. Int J Solids Structures, vol. 35, 1998. p. 4513–5031.
[10] Thimus JF, Abousleiman Y, Cheng AH-D, Coussy O, Detournay E. Poromechanics. A Tribute to Maurice A Biot. In: Proceedings of the Biot Conference on Poromechanics Louvain-la-Neuve. Belgium, The Netherlands: A.A. Balkema; 1998.
[11] Lewis RW, Schrefler BA. The finite element method in the static and dynamic deformation and consolidation of porous media. New York: John Wiley; 1998.
[12] de Boer R. Theory of porous media. Berlin: Springer-Verlag; 2000.
[13] Auriault J-L, Geindreau C, Royer P, Bloch J-F, Boutin C, Lewandowska J, editors. Poromechanics II Proceedings of the Second Biot Conference on Poromechanics. Grenoble, France, The Netherlands: A.A. Balkema; 2002.
[14] Chen W-F. Limit analysis and soil plasticity. In: Developments in geotechnical engineering, vol. 7. Amsterdam: Elsevier Science Publishing Company; 1975.
[15] Desai CS, Siriwardane HJ. Constitutive laws for engineering materials with emphasis on geologic materials. Englewood-Cliffs, NJ: Prentice-Hall; 1984.
[16] Prevost J-H. Dynamics of porous media. In: Sayed SM, editor. Geotechnical modeling and applications. Houston: Gulf Publishing Company; 1987. p. 76–146 [Chapter 3].
[17] Borja RI. Elasto-plastic consolidation at finite strain. Computer methods and advances in geomechanics. In: Siriwardane HJ, Zaman MM, editors. Proceedings of the Eighth International Conference on Computer Methods in Advanced Geomechanics, Morgantown, WVa, vol. 1. The Netherlands: A.A. Balkema; 1994. p. 753–8.
[18] Davis RO, Selvadurai APS. Plasticity and geomechanics. Cambridge: Cambridge University Press; 2002.
[19] de Boer R, Ehlers W. On the problem of fluid and gas-filled elasto-plastic soils. Int J Solids Struct 1986;22:1231–42.
[20] de Boer R, Ehlers W. Uplift, friction, and capillarity; three fundamental effects for liquid-saturated porous solids. Int J Solids Struct 1990;26:43–51.
[21] Cook NGW. Failure of rock. Int J Rock Mech Min Sci Geomech Abstr 1965;2:389–403.
[22] Bieniawski ZT, Denkhaus HG, Vogler UW. Failure of fractured rock. Int J Rock Mech Min Sci Geomech Abstr 1969;6:323–46.
[23] Paterson MS. Experimental rock deformation – the brittle field. Vienna, Austria: Springer-Verlag; 1978.
[24] Martin CD, Chandler NA. The progressive fracture of Lac du Bonnet granite. Int J Rock Mech Min Sci Geomech Abstr 1994;31:643–59.

[25] Chau KT, Wong RHC. Effective moduli of micro-cracked rocks: theories and experimentation. Int J Damage Mech Geomech Abstr 1997;6:258–77.
[26] Tang CA, Tham LG, Lee PKK, Yang TH, Li LC. Coupled analysis of flow, stress and damage (FSD) in rock failure. Int J Rock Mech Min Sci Geomech Abstr 2002; 39:477–89.
[27] Zoback MD, Byerlee JD. The effect of micro-crack dilatancy on the permeability of westerly granite. J Geophys Res 1975;80: 752–5.
[28] Shiping L, Yushou L, Yi L, Zhenye W, Gang Z. Permeability-strain equations corresponding to the complete stress–strain path of Yinzhuang Sandstone. Int J Rock Mech Min Sci Geomech Abstr 1994;31:383–91.
[29] Kiyama T, Kita H, Ishijima Y, Yanagidani T, Akoi K, Sato T. Permeability in anisotropic granite under hydrostatic compression and tri-axial compression including post-failure region. In: Proceedings of the Second North American Rock Mechanics Symposium, 1996. p. 1643–50.
[30] Coste F, Bounenni A, Chanchole S, Su K. A method for measuring hydraulic and hydromechanical properties during damage in materials with low permeability, G.3S. Ecole Polytechnique. Palaiseau; 2001 (Unpublished Report).
[31] Selvadurai APS. Stationary damage modelling of poroelastic contact Int J Solids Struct 2004;41:2043–64.
[32] Cheng H, Dusseault MB. Deformation and diffusion behaviour in a solid experiencing damage: a continuous damage model and its numerical implementation. Int J Rock Mech Min Sci Geomech Abstr 1993;30:1323–31.
[33] Mahyari AT, Selvadurai APS. Enhanced consolidation in brittle geomaterials susceptible to damage. Mech Cohes-Frict Mater 1998;3:291–303.
[34] Shirazi A, Selvadurai APS. Indentation of a poroelastic halfspace susceptible to damage. In: Proceedings of the Canadian Conference on Civil Engineering, Montreal, Paper No. GES 020; 2002, 10 pp.
[35] Mandel J. Etude mathématique de la consolidation des sols. In: acts du colloque international de mécanique, Poitier, France, vol. 4, 1950. p. 9–19.
[36] Mandel J. Consolidation des sols (étude mathématique). Geotechnique 1953;3:287–99.
[37] Cryer RW. A comparison of three-dimensional theories of Biot and Terzaghi. Q J Mech Appl Math 1963;16:401–12.
[38] Rice JR, Rudnicki W, Simons DA. Deformation of spherical cavities and inclusions in fluid-infiltrated elastic materials. Int J Solids Struct 1978;14:289–303.
[39] de Josselin de Jong G. Consolidation around pore pressure meters. J Appl Phys 1953;24:922–8.
[40] de Josselin de Jong G. Application of stress functions to consolidation problems. In: Proceedings of the Fourth International Conference on Soil Mechanics Foundation Engineering, vol. 3. Butterworths: London; 1957. p. 321–3.
[41] Gibson RE, Knight K, Taylor PW. A critical experiment to examine theories of three-dimensional consolidation. In: Proceedings of the European Conference on Soil Mechanics and Foundation Engineering, vol. 1, 1963. p. 69–76.
[42] Verruijt A. Discussion. Sixth Int Conf Soil Mech Fdn Eng 1965;3:401–2.
[43] Selvadurai APS, Shirazi A. Pressure decay in a fluid inclusion located in a damage sensitive poroelastic solid. In: Auriault J-L, Geindreau C, Royer P, Bloch J-F, Boutin C, Lewandowska J, editors. Poromechanics II, Proceedings of the Second Biot Conference in Poromechanics, Grenoble, France. The Netherlands: A.A. Balkema; 2002. p. 933–9.
[44] Skempton AW. The pore pressure coefficients A and B. Geotechnique 1954;4:143–7.
[45] Rice JR, Cleary MP. Some basic stress diffusion solutions for fluid-saturated elastic porous media with compressible constituents. Rev Geophys Space Phys 1976;14:227–41.
[46] Altay GA, Dokmeci MC. A uniqueness theorem in Biot's poroelasticity theory. J Appl Math Phys (ZAMP) 1998;49:838–47.
[47] Kachanov LM. Time of rupture process under creep conditions. Isv Akad Nauk SSR Otd Teck 1958;8:26–31.
[48] Bazant ZP. Mechanics of distributed cracking. Appl Mech Rev 1986;39:675–705.
[49] Simo JC, Ju JW. Strain- and stress-based continuum damage models-II. Int J Solids Struct 1987;23:841–69.
[50] Chow CH, Wang J. An anisotropic theory of elasticity for continuum damage mechanics. Int J Fract 1987;33:3–16.
[51] Ju JW. Isotropic and anisotropic damage variables in continuum damage mechanics. J Engng Mech ASCE 1990;116:2764–9.
[52] Lemaitre J, Chaboche JL. Mechanics of solid materials. Cambridge: Cambridge University Press; 1990.
[53] Selvadurai APS, Hu J. The axial loading of foundations embedded in frozen soils. Int J Offshore Polar Eng 1996;6:96–103.
[54] Krajcinovic D. Damage mechanics. Amsterdam: North-Holland; 1996.
[55] Voyiadjis GZ, Ju JW, Chaboche JL, editors. Damage mechanics in engineering materials. Studies in applied mechanics. Amsterdam, The Netherlands: Elsevier Science; 1998. p. 46.
[56] Lemaitre J. How to use damage mechanics. Nucl Eng Des 1984;8:233–2454.
[57] Sandhu RS, Wilson EL. Finite element analysis of flow in saturated porous media. J Eng Mech Div ASCE 1969;95(EM3):641–52.
[58] Booker JR, Small JC. An investigation of the stability of numerical solution of Biot's equations of consolidation. Int J Solids Struct 1975;11:907–17.
[59] Verruijt A. The generation and dissipation of pore pressures. In: Gudehus G, editor. Finite elements in geomechanics. New York: John Wiley; 1977. p. 293–317.
[60] Selvadurai APS, Nguyen TS. Computational modelling of isothermal consolidation of fractured media. Comp Geotech 1995;17:39–73.
[61] Duncan JM, Chang CY. Nonlinear analysis of stress and strain in soils. J Soil Mech Fdn Div 1970;96(SM5):1629–53.
[62] Chen W-F, Saleeb AF. In: Constitutive equations for engineering materials, vol. 1. New York: John Wiley; 1982.
[63] Schulze O, Popp T, Kern H. Development of damage and permeability in deforming rock salt. Engng Geol 2001;61:163–80.
[64] Zhu W, Wong T-F. Transition from brittle faulting to cataclastic flow: permeability evolution. J Geophys Res 1997;102:3027–41.
[65] Zienkiewicz OC, Taylor RL. The finite element method. Fluid mechanics, vol. 2. Oxford: Butterworth-Heinemann; 2000.
[66] Rudnicki JW. Plane strain dislocations in linear elastic diffusive solids. J Appl Mech 1987;54:545–52.